NANO-ORGANIZED STRUCTURES IN A FIELD: EQUILIBRIUM AND STEADY-STATE GRADIENT FOCUSING IN MULTICOMPONENT COLLOIDAL SYSTEMS

Josef JANČA

Université de La Rochelle, Pôle Sciences et Technologie,
Avenue Michel Crépeau 17042 La Rochelle Cedex 01, France; e-mail: jjanca@univ-lr.fr

Received March 26, 2001
Accepted August 7, 2001

Focusing behaviour appearing in multicomponent colloidal systems exposed to the action of a field can be considered as a special case of the formation of the organized structures on a nanosize scale. The emergence of such structures was observed under the thermodynamic equilibrium conditions as well as at a steady state characterized by an entropy production due to an energy flux. It has already been proven that a complex liquid forming a primary concentration gradient should not necessarily behave as a continuum with respect to the focused species but the focusing effect can appear as well. Two theoretical models predicting equilibrium or steady-state gradient focusing under various conditions were published recently. The first model is based on a macroscopic dynamic mechanism and the other on a microscopic kinetic mechanism. Although seemingly complementary, they bring along some paradoxes. The dynamic model describes correctly the focusing of the large species in a continuum or pseudocontinuum gradient. Nevertheless, its application to the description of the focusing emerging in a bidisperse or multicomponent mixture of the colloidal particles of commensurable sizes does not seem to be physically adequate. The kinetic model provides a coherent physical image of the focusing in such a bidisperse or multicomponent mixture but, on the other hand, it gives rise to the mentioned paradoxes. In this study, both models were compared with the former theoretical approaches dealing with equilibrium or steady states established in multicomponent and/or concentrated colloidal systems interacting with a field. Moreover, computer simulation was carried out to elucidate the consequences of the mentioned paradoxes and to discuss the domain of the prevailing contribution of the macroscopic and microscopic mechanisms to the resulting focusing phenomenon.

Keywords: Suspensions; Colloids; Transport phenomena; Sedimentation; Centrifugation; Gradient focusing; Macroscopic and microscopic focusing forces.

Transport phenomena generated by the interactions of physical or chemical field forces with the colloidal species cause a wide scope of unresolved problems of fundamental importance. Some of them are related to the transient state, characterized by non-zero macroscopic mass and energy fluxes. The other concern the equilibrium or steady states for which the macro-

scopic mass fluxes are zero and the macroscopic energy flux is zero under equilibrium conditions at constant temperature but not necesarily in a steady state[1]. Although the macroscopic equilibrium or steady states are assumed to correspond to a maximum number of possible adequate microstates, it has to be stressed that these microscopic states fluctuate around their averages due to the dynamics of the thermal molecular motion which was intuitively assumed as chaotic in spite of the deterministic character of the macroscopic phenomena. This assumption has only recently been proven by experiments[2].

The extensive studies of the transient state (see refs[3,4] and other references cited therein) and of the equilibrium or steady state in colloidal systems exposed to the effect of gravitational, centrifugal and electric fields allowed to reveal a paradox concerning the macroscopic and microscopic approaches to explain the focusing phenomenon, to elaborate a theoretical model of the focusing coherent with our previous experiments and to prognosticate the focusing effect not yet observed experimentally (see refs[5–7] and other references cited therein). In this paper, our theoretical model is further developed to refine its important aspects remaining not fully argued with regard to the former theories and to elucidate, by computer simulation, the major consequences of the paradoxes between the dynamic and kinetic mechanisms.

THEORY

Chemical Potential in a Field

The equilibrium or steady-state focusing phenomenon can appear in a multicomponent colloidal suspension due to the effective property gradient generated by the interaction of a field with the components of such a complex liquid. The change in energy due to the macroscopic scale transport (from a location 1 to a location 2) of uniform colloidal species k, dispersed in a simple liquid and exposed to a field associated with a potential Ψ is[1]:

$$\mathrm{d}U = T\mathrm{d}S - p\mathrm{d}V + \Psi_1 \sum_k \tau_k \mathrm{d}N_{1k} + \Psi_2 \sum_k \tau_k \mathrm{d}N_{2k} + \sum_k \mu_{1k} \mathrm{d}N_{1k} + \sum_k \mu_{2k} \mathrm{d}N_{2k} \,, \quad (1)$$

where $\mathrm{d}N$ is the mole number change, μ is the chemical potential and the product $\tau\Psi$ has the meaning of the energy of interaction per mole of the transported colloidal species. Thus the change in entropy can be written:

$$T\mathrm{d}S = \mathrm{d}U + p\mathrm{d}V - \sum_k \left[\left(\mu_{2k} + \tau_k \Psi_2 \right) - \left(\mu_{1k} + \tau_k \Psi_1 \right) \right] \mathrm{d}\mathcal{A}_k \,, \qquad (2)$$

where the advancement is defined as $\mathrm{d}\mathcal{A}_k = \mathrm{d}N_{2k} = -\mathrm{d}N_{2k}$. The chemical potential including the effect of the field, $\tilde{\mu}_k$, is then[1]:

$$\tilde{\mu}_k = \mu_k + \tau_k \Psi \,. \qquad (3)$$

Then Eq. (*4*) holds for an equilibrium between the locations 1 and 2:

$$\Delta\tilde{\mu}_k = \tilde{\mu}_{1k} - \tilde{\mu}_{2k} = 0 \qquad \text{and} \qquad \Delta\mu_k = -\tau_k \Delta\Psi \,. \qquad (4)$$

Equation (*4*) holds not only for an equilibrium between the locations 1 and 2 but for any intermediate positions as well.

Equilibrium in Gravitational or Centrifugal Field

An equilibrium established in a suspension of ideal colloidal particles exposed to the effect of a gravitational or centrifugal field can be described by analogy with the well-known barometric formula for the molecules of an ideal gas. The coupling constant τ is, in the case of ideal gas, the molar mass M_k and $\Psi = -xg$, where x is the position in the direction parallel but opposite to the field action and g is the gravitational or centrifugal acceleration considered a constant to simplify the calculations; otherwise its variation throughout the system has to be taken into account. Then

$$\mu_k(x) = \mu_k(0) - xM_k g \qquad (5)$$

and

$$\mu_k(x) = \mu_k(T) + RT \ln \left[a_k(x)/a_k(0) \right] \,, \qquad (6)$$

where a_k is the activity which can be approximated by the molar concentration c_{M_k}, R is gas constant and T is the temperature. As a result:

$$c_{M_k}(x) = c_{M_k}(0)\exp\left(-\frac{xM_k g}{RT}\right). \quad (7)$$

Equation (*7*) can be generalized for a suspension of colloidal species by considering a force F_k of any physical field acting on one particle or molecule having the effective mass m_k:

$$c_k(x) = c_k(0)\exp\left(-\frac{xF_k}{k_B T}\right), \quad (8)$$

where k_B is Boltzmann constant and $c_k(x)$ and $c_k(0)$ are the mass concentrations. Provided that the suspending liquid can be considered as a continuum with regard to the size of the colloidal species, the effective mass is:

$$m_k = v_k(\rho_k - \rho_l) = v_k\Delta\rho_k\,, \quad (9)$$

where v_k is the volume of one colloidal particle, ρ_k is its mass density and ρ_l is mass density of the suspending liquid. Equation (*8*) is based on purely thermodynamic considerations. However, the identical result can be obtained from the mass fluxes balance. When neglecting the dependence of the transport coefficients U_k (sedimentation velocity) and D_k (diffusion coefficient) on the concentration, the flux J_k of the species k, sedimenting in the direction of the field action (x-coordinate) can be written as:

$$J_k = -D_k\frac{\partial c_k}{\partial x} - U_k c_k\,. \quad (10)$$

In the dynamic equilibrium on a macroscopic scale:

$$J_k = \frac{\partial c_k}{\partial \tau} = 0\,. \quad (11)$$

The solution of Eq. (*11*) is:

$$c_k(x) = c_k(0)\exp\left(-\frac{xU_k}{D_k}\right) \quad (12)$$

which is exactly the same relationship as Eq. (*8*) because

$$\frac{U_k}{D_k} = \frac{F_k}{k_B T}. \qquad (13)$$

Equation (*12*) was already derived by Einstein[8,9] and verified experimentally by Perrin[10]. The concentration $c_k(0)$ in Eq. (*12*) can be substituted by calculating the average concentration, $c_{k,ave}$:

$$c_{k,ave} = \frac{\int_0^h c_k(x)\mathrm{d}x}{\int_0^h \mathrm{d}x} = c_k(0)\frac{D_k}{hU_k}\left(1 - \exp\left(-\frac{hU_k}{D_k}\right)\right), \qquad (14)$$

where h is the thickness of the liquid layer it the direction of the x-axis. The result is:

$$c_k(x) = \frac{c_{k,ave} hU_k}{D_k\left(1 - \exp\left(-hU_k / D_k\right)\right)} \exp\left(-\frac{xU_k}{D_k}\right). \qquad (15)$$

Although derived specifically for sedimentation equilibrium in gravitational or centrifugal field, the above relationships can generally be used to describe equilibrium or steady-state mass flux balance independently of the nature of the applied field.

Sedimentation Equilibrium in Concentrated Colloidal Suspensions

The validity of Eqs (*8*), (*12*) and (*15*) is limited to the range of low concentrations. The theoretical equilibrium distribution in concentrated suspensions of uniform-size colloidal particles exposed to the action of the gravitational or centrifugal field was derived by Vrij[11] who obtained the function volume fraction, ϕ, *versus* position, ξ, based on the Percus–Yevick[12,13] (PY) or Carnahan–Starling[14] (CS) dependence of the osmotic pressure on the volume fraction of the hard sphere suspensions. The resulting function is represented by the curve *1* in Fig. 1. This curve corresponds to PY as well as CS models and the curve *2* to Eqs (*8*), (*12*) and (*15*). The curve *2* was obtained by inverting Eq. (*8*) and by transforming the variable x into ξ according to ref.[11] in order to obtain the comparable plots. Consequently, the ξ-coordinate is dimensionless and its positive direction is inverted in comparison with the above defined variable x. Moreover, an arbitrarily chosen integration constant, which cannot be calculated analytically due to the

transcendental character of the ϕ *versus* ξ function, obtained by Vrij[11], must be added to x to obtain ξ (see ref.[11] for details). It can be seen in Fig. 1 that a satisfactory agreement between the curves *1* and *2* exists only up to the volume fraction $\phi \leq 0.05$. An inflection point on the sigmoidal curve *1* corresponds to $\phi \approx 0.13$. Regardless of the considerable differences between the curves *1* and *2* above $\phi > 0.05$, none of the two models is appropriate to predict the occurrence of the focusing phenomena in bidisperse or multicomponent colloidal suspensions.

Sedimentation Equilibrium in Multicomponent Systems

Vrij[11] described sedimentation equilibrium in a multicomponent system with one solvent and p colloidal species labeled 0, 1, 2, ...q. His fundamental differential equation relates the variation of a measurable property, such as the refractive index n, of a colloidal suspension to the properties of the system and the operational variables:

$$-\left(\frac{\mathrm{d}(n-n_0)}{\mathrm{d}r}\right)\left(\frac{1}{r\omega^2}\right) = \sum_{i=1}^{q}\sum_{j=1}^{q}\left(\frac{\partial n}{\partial c_{Ni}}\right)_{pc_N^*}\left(\frac{\partial \rho_s}{\partial c_{Nj}}\right)_{pc_N^*}\left(\frac{\partial c_{Ni}}{\partial \mu_j}\right)_{\mu}, \qquad (16)$$

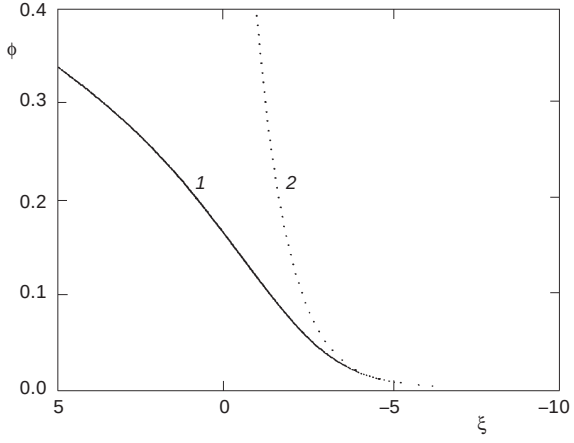

FIG. 1
Distribution of the volume fraction ϕ as a function of the dimensionless position ξ in sedimentation equilibrium calculated by using the Percus–Yevick or Carnahan–Starling dependence of osmotic pressure on ϕ (curve *1*) or from Eqs (*8*), (*12*) or (*15*) (curve *2*)

where r is the distance from the axis of the rotation, ω is the angular velocity of the rotation, ρ_s is the density of the suspension, c_{Ni} is the concentration of the colloidal species i expressed as the number of particles per unit volume, and the subscript pc_N^* implies that the pressure p and the $c_{Ni} \neq c_{Nj}$ are held constant (with $i, j = 1, 2, ...q$). As pointed out by Vrij[11], the derivatives $\partial c_{Ni}/\partial \mu_j$ are theoretically not readily available. This means that whereas the solution of Eq. (*16*) provides a possibility to calculate a global concentration distribution of all species in sedimentation equilibrium as, for example, a variation of a mentioned measurable property, it does not allow a detailed look into the concentration distribution of each particular species.

It has generally been regarded as axiomatic that an ideal bidisperse or multicomponent colloidal suspension composed of two or several uniform but different size particle populations in sedimentation equilibrium displays a simple superposition of the particular exponential concentration distributions each satisfying Eq. (*15*). Therefore, two independent concentration distributions concerning an equilibrium established in a bidisperse colloidal suspension with no correlations are schematically demonstrated in Fig. 2. The conclusion resulting from such an axiom is that none the sedimenting species of different molar masses (or different sizes) can focus but each exhibits its proper exponential concentration distribution. Never-

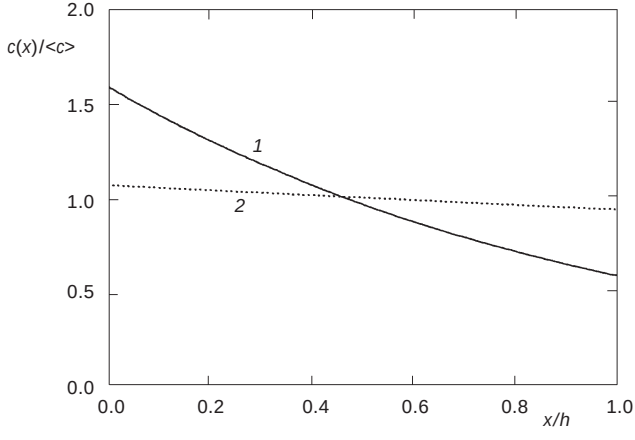

FIG. 2
Dimensionless concentration distributions $c(x)/\langle c \rangle$ as a function of the dimensionless position x/h in sedimentation equilibrium calculated from Eq. (*15*) for a mixture of two different-size particle populations, denoted as *1* and *2*, of the size (diameter) ratio $d_1/d_2 = 2$ with no correlations

theless, it has already been demonstrated theoretically as well as experimentally[5–7,15–23] that this axiom is not correct.

Soon after our first theoretical and experimental studies of equilibrium and steady-state gradient focusing phenomena[15–17], Biben *et al.*[24] published a theoretical description of the concentration distribution established in the concentrated colloidal suspensions in sedimentation equilibrium. Their model is based on two different approaches, the local density approximation and Monte Carlo simulations. An interesting result was obtained by Monte Carlo simulation of a sedimentation equilibrium in a suspension of uniform size particles. Concentration profile in equilibrium exhibited the damped oscilations near the bottom of the sedimentation cell thus indicating a pronounced layering up to the altitude corresponding roughly to few to 15 particle diameters under the imposed conditions of the simulation. An exactly solvable one-dimensional model of a concentration distribution in an external field derived already by Percus[25] and solved for a particular case of N_{HR} hard rods confined between two hard walls[26,27] was used by Biben *et al.*[24] to obtain the relationship applicable to the particular case of the concentration profile of the hard rods exposed to the action of the gravitational field:

$$c(x) = \alpha \sum_{j=0}^{j_0(z)} \frac{N_{HR}!}{(N_{HR} - j - 1)!\, j!} \frac{\left(\exp[\alpha(z - j\sigma)] - 1\right)^j}{\exp[\alpha N_{HR}(z - j\sigma)]} \qquad (17)$$

and

$$j_0(z) = \mathrm{Int}\left(\frac{z}{\sigma}\right) \quad \text{if} \quad z < (N_{HR} - 1)\sigma \quad \text{and} \qquad (18)$$
$$j_0(z) = N_{HR} - 1 \quad \text{if} \quad z > (N_{HR} - 1)\sigma,$$

where N_{HR} is the number of hard rods of the length σ and effective mass m_{HR}, and $\alpha = m_{HR}g/k_BT$. The calculated equilibrium concentration distribution exhibits, as in the above mentioned case of Monte Carlo simulations, the damped oscilations near the bottom of the sedimentation cell. From the mathematical viewpoint, the function $c(x)$ given by Eq. (*17*) with the limiting conditions given by Eqs (*18*) has inherently, for conveniently chosen parameters α and/or σ, an oscillatory character. Nevertheless, as far as Monte Carlo simulation carried out by Biben *et al.*[24] exhibits similar oscillatory behaviour, both approaches[24] should suitably represent a physical reality.

The local density approximation and Monte Carlo simulations were used[24] to calculate the concentration distribution in equlibrium of two model bidisperse suspensions containing the same numbers of particles of the same size ratio 2 but either the particles of the same masses or the particles of the same mass densities. In two model cases, one of the particle populations goes through a maximum whereas the other concentrates near the bottom. Nevertheless, in the first case of equal masses, the concentration distribution with a maximum concerns the larger particles while in the case of equal mass densities of the particles, it is the concentration distribution of the smaller particles which exhibits a maximum. Obviously, the calculations performed in ref.[24] did not permit any quantitative conclusion as to the position of the maximum or the width of the focused zone with respect to the imposed operational parameters such as the average volume fraction of each particular species, their volume fraction ratio, *etc.*

Appearance of Gradient Focusing Phenomena

Dynamic and Kinetic Models

From the macroscopic as well as from the microscopic point of view, the species undergoing the gradient focusing phenomena should experience the effect of a position-dependent focusing force $\mathcal{F}_f(x)$ for which Eq. (*19*) holds:

$$\begin{aligned} &\mathcal{F}_f(x) = f(x) && \text{within } 0 < x < h \\ &\mathcal{F}_f(x) = 0 \quad \text{for} \quad x = x_f && 0 < x_f < h \\ &\mathcal{F}_f(x) > 0 \quad \text{for} \quad x < x_f \\ &\mathcal{F}_f(x) < 0 \quad \text{for} \quad x > x_f \ , \end{aligned} \tag{19}$$

where x_f is a position within the system at which the concerned species are focused. The same conditions can casually be written for a velocity of the focused species $\mathcal{U}_f(x)$, generated by the focusing force.

The focusing force resulting from Archimedes' principle in our previous macroscopic dynamic model[15,21] is:

$$\mathcal{F}_f(x) = (\rho(x) - \rho_f) v_f g \ , \tag{20}$$

where ρ_f and v_f are the density and the volume, respectively, of a focused particle. Then for concentration distribution of the focused species in sedimentation equilibrium[15,21], Eq. (*21*) holds

$$c_f(x) = c_f(x_f)\exp\left\{\left[\frac{v_f g_f \phi_{m,ave} \Delta\rho_m h}{k_B T\left(1-\exp\left(-hF_{I,m}/k_B T\right)\right)}\right]\times \left[\exp\left(-x_f F_{I,m}/k_B T\right) - \exp\left(-xF_{I,m}/k_B T\right) + \exp\left(-x_f F_{I,m}/k_B T\right)\left(\frac{F_{I,m}\left(x_f - x\right)}{k_B T}\right)\right]\right\}, \quad (21)$$

where $\phi_{m,ave}$ is the average volume fraction of a gradient forming (modifier) species (particles), $\Delta\rho_m$ is the density difference between the modifier particles and the suspending liquid, g_f is the acceleration generated by a field interacting with focused species, and $F_{I,m}$ is the force acting on the modifier particle which is proportional to its volume in the case of gravitational or centrifugal field. Equation (*21*) applies specifically to the so-called isopycnic focusing but it can be easily generalized to be applicable to any gradient focusing[28]. It is worth noting that the force $F_{I,m}$ and the acceleration g_f can be both produced by a single field interacting with modifier as well as with the focused species but also by the action of two fields each interacting independently with modifier and focused colloidal species.

Our previous microscopic kinetic model[5,6] assumed that the concentration distribution of the modifier particles (generated by a primary field) creates a gradient of the partial osmotic pressure which produces a unidirectional and position-dependent expelling force acting on a focused spherical particle which is displaced to the extreme limit of the system. This expelling or "lift" force $F_f(x)$, which is due to the difference between the integral osmotic pressures on the upper and lower hemispheres of a focused particle, has been calculated previously[5]. It has been concluded that $F_f(x)$ must be counteracted by a force $F_{II,f}$ to yield the focusing force $\mathcal{F}_f(x)$ satisfying the conditions imposed by Eqs (19). As a result, the force $\mathcal{F}_f(x)$ can be composed of at least three contributions:

$$\mathcal{F}_f(x) = F_f(x) - F_{II,f} \pm F_{I,f}\,, \quad (22)$$

the surface force $F_f(x)$ resulting from the interactions between the focused and gradient-forming modifier particles, the volume force $F_{I,f}$ which can be generated by the primary field due to the macroscopic effective property of

the suspending liquid, and the force $F_{II,f}$ due to the secondary field. The concentration distribution of the focused species derived for the kinetic model was[5,6]:

$$c_f(x) = c_f(0)\exp\left\{\frac{2\pi r_f k_B T c_{m,ave} h f(r_f)}{m_m F_{I,m}\left(1-\exp\left(-hF_{I,m}/k_B T\right)\right)}\left[1-\exp\left(-xF_{I,m}/k_B T\right)\right] - \frac{xF_{II,f}}{k_B T}\right\}, \quad (23)$$

where $F_{I,f} = 0$ and the function $f(r_f)$ results[5] from the calculation of the expelling force $F_f(x)$ acting on a focused particle of a radius r_f:

$$f(r_f) = [\exp(-r_f F_{I,m}/k_B T) + \exp(r_f F_{I,m}/k_B T) - 2]\,. \quad (24)$$

In comparison with Eq. (*24*) in ref.[5], the above Eq. (*23*) was obtained by integration of Eq. (*23*) from ref.[5] with respect to $x = 0$. The concentrations $c_f(0)$ and $c_f(x_f)$ at the position of the focused zone x_f are not known *a priori*. However, for previous Eq. (*24*) in ref.[5] as well as for the above Eq. (*23*), the normalization condition

$$c_{f,ave} = \frac{1}{h}\int_0^h c_f(x)\,dx \quad (25)$$

allows to eliminate the mentioned concentrations by calculating the average concentration $c_{f,ave}$ which is equal to the initial uniform concentration of the focused species.

A crucial difference between the dynamic and kinetic models is that the $\mathcal{F}_f(x)$ is purely volume force in the first case (see Eq. (*20*)), whereas it is composed of surface force $F_f(x)$ and of $F_{I,f}$ and $F_{II,f}$ which can be either volume or surface forces in the other case (see Eq. (*22*)), according to the nature of the effective field which generates the corresponding force. In the following paragraphs, we will analyze the above described dynamic and kinetic theoretical approaches, represented by Eqs (*21*) and (*23*).

COMPUTER SIMULATION

Dynamic Model

A detailed computer simulation analysis of Eq. (*21*) corresponding to the dynamic macroscopic model applied to a bidisperse mixture of two different but uniform sizes particle populations was performed previously[21]. Figure 3 demonstrates the most important results which can be summarized as follows.

The density gradient formed under the imposed conditions (given in the caption for Fig. 3), which represents a real case of the sedimentation in a centrifugal field, is shown in Fig. 3a. Its exponential shape corresponds to Eq. (*15*) where the concentrations were recalculated to give the mass density dependence $\rho(x)$.

Figures 3b and 3c show the shapes of the focused zones (means the concentration distributions of the focused species) where the size ratio of the focused to the density gradient-forming (modifier) particles is $d_f/d_m = 30$ in the case shown in Fig. 3b and $d_f/d_m = 6$ in Fig. 3c. The positions of the maxima of the focused zones I and II are determined by the imposed densities of the concerned species. It is evident from both Figs 3b and 3c that the width of the focused zones increases from the zones I to II with the decreasing steepness of the local density gradient in Fig. 3a. The zone width increases with the decreasing size ratio d_f/d_m as can be seen in Figs 3b and 3c. All focused zones are asymmetrical; however, this fact is more evident, especially for broader zones, in Fig. 3c. Experimental studies[7,20,22] confirmed these theoretical predictions. The identical behaviour was observed when the focusing was generated by a single centrifugal field force as well as by a coupled action of the electric and gravitational fields. This observation justifies the generalization of our concept to all systems where the interaction of a field with a dispersed matter can produce transport phenomena, independently of the considered model and of the nature of the fields.

As a result, the dynamic model clearly indicates that the focusing phenomenon of large particles should appear in a bidisperse suspension of colloidal particles even if the particle size ratio is low and the density gradient-forming particles suspended in a liquid can no longer be considered a continuum with regard to the focused species. The focusing disappears only when the size ratio approaches to 1. Nevertheless, this model does not consider the individual microscopic scale interactions between the concerned gradient-forming and focused species or the probability of these

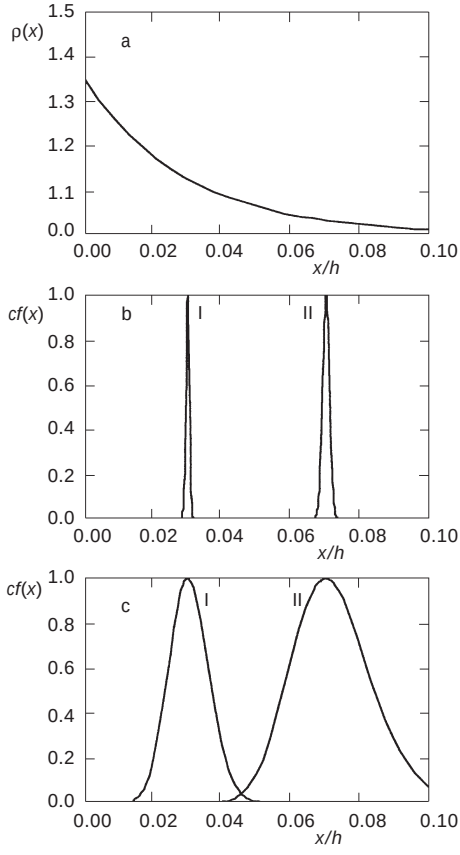

FIG. 3

Equilibrium and steady-state concentration distributions in a bidisperse mixture of two different but uniform-size particle populations interacting independently with two fields of different nature but identical strengths. a Density distribution $\rho(x)$ as a function of the dimensionless position x/h of the modifier particles calculated from Eq. (*15*) after tranformation of the concentrations to the densities by $\rho(x) = c(x) - \rho_l$, where ρ_l is the density of a suspending liquid. The operational parameters were: diameter of the modifier particles d_m = 30 nm, $F_{I,m} = \pi\Delta\rho_m d_m^3/6 g_f$ (g_f = 98 100 cm s^{-2}), $\phi_{m,ave}$ = 0.1, h = 0.1 cm, $\Delta\rho_m$ = 1 g cm^{-3}. b Equilibrium or steady-state concentration distributions calculated from Eq. (*21*) for two different masses but identical sizes (curves I and II) of the focused particles in the modifier concentration gradient shown in Fig. 3a. The operational parameters were as in Fig. 3a, g_f = 98 100 cm s^{-2}, particle size ratio d_f/d_m = 30. c Equilibrium or steady-state concentration distributions calculated from Eq. (*21*) for two different masses but identical sizes (curves I and II) of the focused particles in the modifier concentration gradient shown in Fig. 3a. The operational parameters were as in Fig. 3a, g_f = 98 100 cm s^{-2}, particle size ratio d_f/d_m = 6

events which, at least whenever the size of gradient-forming and focused species is commensurable, should dominate the focusing phenomenon.

Kinetic Model

The results of computer simulation analysis of Eq. (*23*) are demonstrated in Fig. 4. The imposed operational conditions, given in the caption to Fig. 4, correspond again to a physically real case of sedimentation in a centrifugal field and are, in fact, the same in Figs 4a and 4b as those given for simulations shown in Fig. 3. The concentration (or density) gradient of the modifier particles shown in Fig. 3a corresponds also to the situations demonstrated in Fig. 4. The concentration distribution of the focused species calculated from Eq. (*23*) (curve III in Fig. 4a), is substantially broader compared with the focused zones corresponding to the calculations using Eq. (*21*) (curves I and II in Fig. 4a). It has to be stressed that the positions of the maxima of all curves I, II, and III are imposed by the arbitrarily chosen x_f values in the case of Eq. (*21*) and $F_{I,f}$ and $F_{II,f}$ values in the case of Eqs (*23*) and (*22*), respectively. The width of the focused zone calculated from Eq. (*23*) increases with the decreasing size ratio d_f/d_m as can be seen from Figs 4a and 4b, curves III. For comparison, curves I and II corresponding to the dynamic model were reproduced from Fig. 3. Curve IV also corresponds to the dynamic model (Eq. (*21*)) and its maximum has the same position as that of curve III. Finally, Fig. 4c shows the result of a computer simulation in the case when the primary and secondary fields have not the same strengths. The secondary field interacting only with the focused species was three times stronger than the primary field interacting only with modifier species. Such a case corresponds to a situation when two fields of different nature can (but should not) interact differently with the primary gradient-forming modifier and with the focused species. Compared with Fig. 4b, all focused zones in Fig. 4c are narrower due to the stronger secondary field interacting only with the focused species. The primary field interacting only with modifier species has the same strength in all cases demonstrated in Fig. 4. As a result, general tendency of the dependence of the width of the focused zone on the operational parameters is the same for both models.

CONCLUSION

Comparison of our theoretical models with the former theories of sedimentation has clearly demonstrated that the prediction of the appearance of the focusing phenomena is very precise when applying these models. Com-

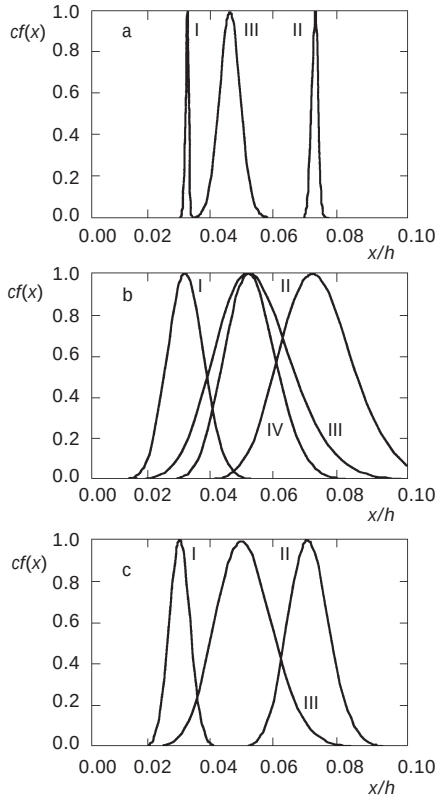

FIG. 4

Equilibrium or steady-state concentration distributions in a bidisperse mixture of two different but uniform-size particle populations interacting independently with two fields of different nature. a Equilibrium or steady-state concentration distributions of the focused particles calculated from Eq. (*23*) (curve III). The concentration gradient of the modifier particles is the same as that shown in Fig. 3a. The operational parameters were: diameter of the modifier particles d_m = 30 nm, $F_{I,m} = \pi\Delta\rho_m d_m^3/6g_f$ (g_f = 98 100 cm s^{-2}), $F_{II,f} = \pi\Delta\rho_f d_f^3/6g_f$ (g_f = 98 100 cm s^{-2}), $F_{I,f}$ = 0, $\phi_{m,ave}$ = 0.1, h = 0.1 cm, $\Delta\rho_m$ = 1 g cm^{-3}, particle size ratio d_f/d_m = 30. Curves I and II were taken from Fig. 3b for comparison. b Equilibrium or steady-state concentration distributions of the focused particles calculated from Eq. (*23*) (curve III). The concentration gradient of the modifier particles is the same as that shown in Fig. 3a. The operational parameters were as in Fig. 4a but the particle size ratio d_f/d_m = 6. Curves I and II were taken from Fig. 3c for comparison, curve IV was calculated like curves I and II from Eq. (*21*) but for the same position x/h as curve III. c Equilibrium or steady-state concentration distribution of the focused particles calculated from Eq. (*23*) (curve III). The concentration gradient of the modifier particles is the same as that shown in Fig. 3a. The operational parameters were as in Fig. 4b but $F_{II,f} = \pi\Delta\rho_f d_f^3/6g_f$ (g_f = 294 300 cm s^{-2}), particle size ratio d_f/d_m = 6. Curves I and II were calculated from Eq. (*21*) for comparison using the same operational parameters as in Fig. 3c but g_f = 294 300 cm s^{-2}

puter simulation analysis confirmed that, although based on different first principles, the macroscopic dynamic and microscopic kinetic models are mutually coherent and correspond to a physical reality. Recent experiments[7] indicated that whenever the size ratio d_f/d_m is high (say 10 or more), the macroscopic dynamic model provides a good agreement between the theoretically calculated concentration distribution of the focused species and the experimental findings. On the other hand, for lower values of the size ratio d_f/d_m (say 6 or lower), an important difference in the widths of the calculated and experimentally determined concentration distributions of the focused species was found. The experimental zones were substantially larger. Although no explicit comparison with the kinetic model was made at that time[7], the results of this study indicate that better agreement should be obtained. As a result, a combined macroscopic-microscopic model should allow to predict the focusing behaviour independently of the concerned domain of the size ratio d_f/d_m. The construction of such a complex model is under development.

REFERENCES

1. Kondepudi D., Prigogine I.: *Modern Thermodynamics*. Wiley and Sons Ltd., Chichester 1998.
2. Gaspard P., Briggs M. E., Francis M. K., Sengers J. V., Gammon R. W., Dorfman J. R., Calabrese R. V.: *Nature* **1998**, *394*, 868.
3. Janča J., Gospodinova N., Le Hen S., Špírková M.: *J. Colloid Interface Sci.* **2000**, *229*, 462.
4. Janča J., Checot F., Gospodinova N., Touzain S., Špírková M.: *J. Colloid Interface Sci.* **2000**, *229*, 423.
5. Janča J.: *Phys. Chem. Chem. Phys.* **2000**, *2*, 2607.
6. Janča J.: *Collect. Czech. Chem. Commun.* **2000**, *65*, 1067.
7. Janča J., Gospodinova N.: *Sep. Purif. Methods* **2000**, *29*, 247.
8. Einstein A.: *Ann. Phys. (Leipzig)* **1906**, *19*, 371.
9. Einstein A. in: *Investigations on the Theory of the Brownian Movement* (R. Fürth, Ed.). Dover Publications, Inc., New York 1956.
10. Perrin J.: *C. R. Acad. Sci.* **1908**, *146*, 967.
11. Vrij A.: *J. Chem. Phys.* **1980**, *72*, 3735.
12. Wertheim M. S.: *Phys. Rev. Lett.* **1963**, *10*, 321.
13. Thiele E.: *J. Chem. Phys.* **1963**, *39*, 474.
14. Carnahan N. F., Starling K. E.: *J. Chem. Phys.* **1969**, *51*, 635.
15. Janča J., Audebert R.: *J. Appl. Polym. Sci.* **1993**, *52*, 63.
16. Janča J., Audebert R.: *Mikrochim. Acta* **1993**, *111*, 163.
17. Janča J., Audebert R.: *J. Liq. Chromatogr.* **1993**, *16*, 2211.
18. Janča J.: *Mikrochim. Acta* **1994**, *112*, 197.
19. Janča J., Audebert R.: *Mikrochim. Acta* **1994**, *113*, 299.
20. Janča J., Špírková M.: *Collect. Czech. Chem. Commun.* **1996**, *61*, 819.
21. Janča J.: *J. Colloid Interface Sci.* **1997**, *189*, 51.
22. Janča J., Gospodinova N.: *Collect. Czech. Chem. Commun.* **1998**, *63*, 155.

23. Janča J., Caron N., Gospodinova N.: *J. Chem. Soc., Faraday Trans.* **1998**, *94*, 2961.
24. Biben T., Hansen J.-P., Barrat J.-L.: *J. Chem. Phys.* **1993**, *98*, 7330.
25. Percus J. K.: *J. Stat. Phys.* **1976**, *15*, 505.
26. Vanderlick T. K., Scriven L. E., Davis H. T.: *Phys. Rev. A: At., Mol., Opt. Phys.* **1986**, *34*, 5130.
27. Vanderlick T. K., Davis H. T., Percus J. K.: *J. Chem. Phys.* **1989**, *91*, 7136.
28. Janča J.: *ACS Symp. Ser.* **1995**, *247*, 21.

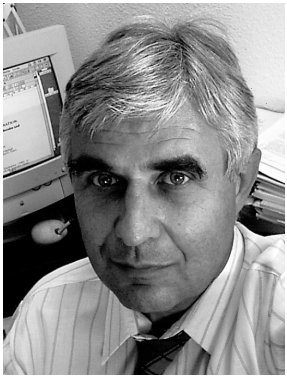

Prof. Ing. Josef Janča, DrSc., born in 1944 in Kroměříž, received MSc grade in Analytical Chemistry (1966) from Institute of Chemical Technology, Prague, Ph.D. degree in Macromolecular Physical Chemistry (1975) from Institute of Macromolecular Chemistry, Czechoslovak Academy of Sciences (CAS), Prague, and DSc degree in Physical Chemistry (1984) from Institute of Chemical Technology, Prague. Author of over 140 original publications, author, co-author, contributor and editor of several books and Encyclopedia, co-editor of Int. J. Polym. Anal. Charact. and member of Editorial Boards of 5 other international scientific journals and encyclopedia. Head of the Laboratory at the Institute of Macromolecular Chemistry CAS in Prague (1975–80), Director of the Institute of Analytical Chemistry CAS in Brno (1980–90), Visiting Associate Professor at the University of Utah, Salt Lake City (1978–79), Visiting Professor at Ecole Supérieure de Physique et Chimie Industrielles, Paris (1990–91) and at Université Pierre et Marie Curie, Paris (1992–1993). He is recently (from 1993) Professor of Physical Chemistry at Université de La Rochelle, France.